

NBDT: NEURAL-BACKED DECISION TREE

Alvin Wan₁, Lisa Dunlap₁^{*}, Daniel Ho₁^{*}, Jihan Yin₁, Scott Lee₁, Suzanne Petryk₁, Sarah Adel Bargal₂, Joseph E. Gonzalez₁

UC Berkeley₁, Boston University₂

{alvinwan, ldunlap, danielho, jihan.yin, scott.lee.3898, spetryk, jegonzal}@berkeley.edu
sbargal@bu.edu

ABSTRACT

Machine learning applications such as finance and medicine demand accurate and justifiable predictions, barring most deep learning methods from use. In response, previous work combines decision trees with deep learning, yielding models that (1) sacrifice interpretability for accuracy or (2) sacrifice accuracy for interpretability. We forgo this dilemma by *jointly improving* accuracy and interpretability using Neural-Backed Decision Trees (NBDTs). NBDTs replace a neural network’s final linear layer with a differentiable sequence of decisions and a surrogate loss. This forces the model to learn high-level concepts and lessens reliance on highly-uncertain decisions, yielding (1) accuracy: NBDTs match or outperform modern neural networks on CIFAR, ImageNet and better generalize to unseen classes by up to 16%. Furthermore, our surrogate loss improves the *original* model’s accuracy by up to 2%. NBDTs also afford (2) interpretability: improving human trust by clearly identifying model mistakes and assisting in dataset debugging. Code and pretrained NBDTs are at github.com/alvinwan/neural-backed-decision-trees.

1 INTRODUCTION

Many computer vision applications (e.g. medical imaging and autonomous driving) require insight into the model’s decision process, complicating applications of deep learning which are traditionally black box. Recent efforts in explainable computer vision attempt to address this need and can be grouped into one of two categories: (1) saliency maps and (2) sequential decision processes. Saliency maps retroactively explain model predictions by identifying which pixels most affected the prediction. However, by focusing on the input, saliency maps fail to capture the model’s decision making process. For example, saliency offers no insight for a misclassification when the model is “looking” at the right object for the wrong reasons. Alternatively, we can gain insight into the model’s decision process by breaking up predictions into a sequence of smaller semantically meaningful decisions as in rule-based models like decision trees. However, existing efforts to fuse deep learning and decision trees suffer from (1) significant accuracy loss, relative to contemporary models (e.g., residual networks), (2) reduced interpretability due to accuracy optimizations (e.g., impure leaves and ensembles), and (3) tree structures that offer limited insight into the model’s credibility.

To address these, we propose **Neural-Backed Decision Trees (NBDTs)** to jointly improve *both* (1) accuracy and (2) interpretability of modern neural networks, utilizing decision rules that preserve (3) properties like sequential, discrete decisions; pure leaves; and non-ensembled predictions. These properties in unison enable unique insights, as we show. We acknowledge that there is no universally-accepted definition of interpretability (Lundberg et al., 2020; Doshi-Velez & Kim, 2017; Lipton, 2016), so to show interpretability, we adopt a definition offered by Poursabzi-Sangdeh et al. (2018): A model is interpretable if a human can validate its prediction, determining when the model has made a sizable mistake. We picked this definition for its importance to downstream benefits we can evaluate, specifically (1) model or dataset debugging and (2) improving human trust. To accomplish this, NBDTs replace the final linear layer of a neural network with a differentiable oblique decision tree and, unlike its predecessors (*i.e.* decision trees, hierarchical classifiers), uses a hierarchy derived from model parameters, does not employ a hierarchical softmax, and can be created from *any* existing classification neural network without architectural modifications. These improvements

^{*}denotes equal contribution

tailor the hierarchy to the network rather than overfit to the feature space, lessens the decision tree’s reliance on highly uncertain decisions, and encourages accurate recognition of high-level concepts. These benefits culminate in joint improvement of accuracy and interpretability. Our contributions:

1. We propose a *tree supervision loss*, yielding NBDTs that match/outperform and out-generalize modern neural networks (WideResNet, EfficientNet) on ImageNet, TinyImageNet200, and CIFAR100. Our loss also improves the *original* model by up to 2%.
2. We propose alternative hierarchies for oblique decision trees – *induced hierarchies* built using pre-trained neural network weights – that outperform both data-based hierarchies (e.g. built with information gain) and existing hierarchies (e.g. WordNet), in accuracy.
3. We show NBDT explanations are more helpful to the user when identifying model mistakes, preferred when using the model to assist in challenging classification tasks, and can be used to identify ambiguous ImageNet labels.

2 RELATED WORKS

Saliency Maps. Numerous efforts (Springenberg et al., 2014; Zeiler & Fergus, 2014; Simonyan et al., 2013; Zhang et al., 2016; Selvaraju et al., 2017; Ribeiro et al., 2016; Petsiuk et al., 2018; Sundararajan et al., 2017) have explored the design of saliency maps identifying pixels that most influenced the model’s prediction. White-box techniques (Springenberg et al., 2014; Zeiler & Fergus, 2014; Simonyan et al., 2013; Selvaraju et al., 2017; Sundararajan et al., 2017) use the network’s parameters to determine salient image regions, and black-box techniques (Ribeiro et al., 2016; Petsiuk et al., 2018) determine pixel importance by measuring the prediction’s response to perturbed inputs. However, saliency does not explain the model’s decision process (e.g. Was the model confused early on, distinguishing between *Animal* and *Vehicle*? Or is it only confused between dog breeds?).

Transfer to Explainable Models. Prior to the recent success of deep learning, decision trees were state-of-the-art on a wide variety of learning tasks and the gold standard for interpretability. Despite this recency, study at the intersection of neural network and decision tree dates back three decades, where neural networks were seeded with decision tree weights (Banerjee, 1990; 1994; Ivanova & Kubat, 1995a;b), and decision trees were created from neural network queries (Krishnan et al., 1999; Boz, 2000; Dancey et al., 2004; Craven & Shavlik, 1996; 1994), like distillation (Hinton et al., 2015). The modern analog of both sets of work (Humbird et al., 2018; Siu, 2019; Frosst & Hinton, 2017) evaluate on feature-sparse, sample-sparse regimes such as the UCI datasets (Dua & Graff, 2017) or MNIST (LeCun et al., 2010) and *perform poorly* on standard image classification tasks.

Hybrid Models. Recent work produces hybrid decision tree and neural network models to scale up to datasets like CIFAR10 (Krizhevsky, 2009), CIFAR100 (Krizhevsky, 2009), TinyImageNet (Le & Yang, 2015), and ImageNet (Deng et al., 2009). One category of models organizes the neural network into a hierarchy, dynamically selecting branches to run inference (Veit & Belongie, 2018; McGill & Perona, 2017; Teja Mullapudi et al., 2018; Redmon & Farhadi, 2017; Murdock et al., 2016). However, these models use *impure leaves* resulting in uninterpretable, stochastic paths. Other approaches fuse deep learning into each decision tree node: an entire neural network (Murthy et al., 2016), several layers (Murdock et al., 2016; Roy & Todorovic, 2016), a linear layer (Ahmed et al., 2016), or some other parameterization of neural network output (Kontschieder et al., 2015). These models see reduced interpretability by using k-way decisions with large k (via depth-2 trees) (Ahmed et al., 2016; Guo et al., 2018) or employing an ensemble (Kontschieder et al., 2015; Ahmed et al., 2016), which is often referred to as a “black box” (Carvalho et al., 2019; Rudin, 2018).

Hierarchical Classification (Silla & Freitas, 2011). One set of approaches directly uses a pre-existing hierarchy over classes, such as WordNet (Redmon & Farhadi, 2017; Brust & Denzler, 2019; Deng et al.). However *conceptual similarity is not indicative of visual similarity*. Other models build a hierarchy using the training set directly, via a classic data-dependent metric like Gini impurity (Alaniz & Akata, 2019) or information gain (Rota Bulo & Kontschieder, 2014; Biçici et al., 2018). These models are instead *prone to overfitting*, per (Tanno et al., 2019). Finally, several works introduce hierarchical surrogate losses (Wu et al., 2017; Deng et al., 2012), such as hierarchical softmax (Mohammed & Umaashankar, 2018), but as the authors note, these methods quickly suffer from major accuracy loss with more classes or higher-resolution images (e.g. beyond CIFAR10). We demonstrate hierarchical classifiers attain higher accuracy *without* a hierarchical softmax.

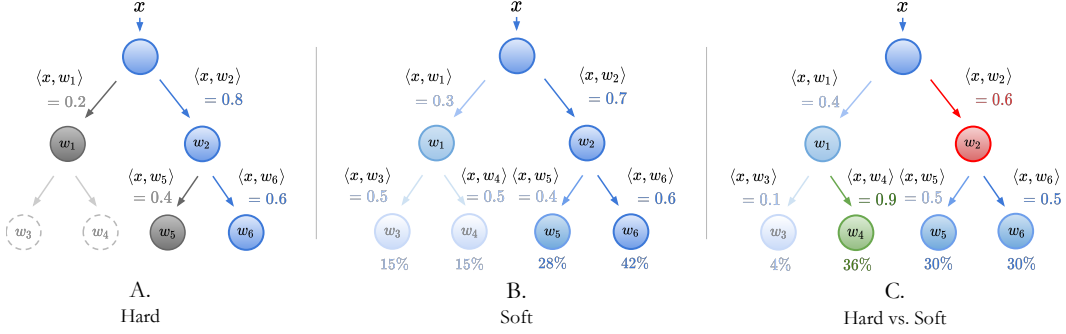


Figure 1: Hard and Soft Decision Trees. **A. Hard:** is the classic “hard” oblique decision tree. Each node picks the child node with the largest inner product, and visits that node next. Continue until a leaf is reached. **B. Soft:** is the “soft” variant, where each node simply returns probabilities, as normalized inner products, of each child. For each leaf, compute the probability of its path to the root. Pick leaf with the highest probability. **C. Hard vs. Soft:** Assume w_4 is the correct class. With hard inference, the mistake at the root (red) is irrecoverable. However, with soft inference, the highly-uncertain decisions at the root and at w_2 are superseded by the highly-certain decision at w_3 (green). This means the model can still correctly pick w_4 despite a mistake at the root. In short, soft inference can tolerate mistakes in highly uncertain decisions.

3 METHOD

Neural-Backed Decision Trees (NBDTs) replace a network’s final linear layer with a decision tree. Unlike classical decision trees or many hierarchical classifiers, NBDTs use path probabilities for inference (Sec 3.1) to tolerate highly-uncertain intermediate decisions, build a hierarchy from pre-trained model weights (Sec 3.2 & 3.3) to lessen overfitting, and train with a hierarchical loss (Sec 3.4) to significantly better learn high-level decisions (e.g., *Animal* vs. *Vehicle*).

3.1 INFERENCE

Our NBDT first featurizes each sample using the neural network backbone; the backbone consists of all neural network layers before the final linear layer. Second, we run the final fully-connected layer as an oblique decision tree. However, (a) a classic decision tree cannot recover from a mistake early in the hierarchy and (b) just running a classic decision tree on neural features drops accuracy significantly, by up to 11% (Table 2). Thus, we present modified decision rules (Figure 1, B):

- 1. Seed oblique decision rule weights with neural network weights.** An oblique decision tree supports only binary decisions, using a hyperplane for each decision. Instead, we associate a weight vector n_i with each node. For leaf nodes, where $i = k \in [1, K]$, each $n_i = w_k$ is a row vector from the fully-connected layer’s weights $W \in \mathbb{R}^{D \times K}$. For all inner nodes, where $i \in [K+1, N]$, find all leaves $k \in L(i)$ in node i ’s subtree and average their weights: $n_i = \sum_{k \in L(i)} w_k / |L(i)|$.
- 2. Compute node probabilities.** Child probabilities are given by softmax inner products. For each sample x and node i , compute the probability of each child $j \in C(i)$ using $p(j|i) = \text{SOFTMAX}(\langle \bar{n}_i, x \rangle)[j]$, where $\bar{n}_i = (\langle n_j, x \rangle)_{j \in C(i)}$.
- 3. Pick a leaf using path probabilities.** Inspired by Deng et al. (2012), consider a leaf, its class k and its path from the root P_k . The probability of each node $i \in P_k$ traversing the next node in the path $C_k(i) \in P_k \cap C(i)$ is denoted $p(C_k(i)|i)$. Then, the probability of leaf and its class k is

$$p(k) = \prod_{i \in P_k} p(C_k(i)|i) \quad (1)$$

In soft inference, the final class prediction \hat{k} is defined over these class probabilities,

$$\hat{k} = \text{argmax}_k p(k) = \text{argmax}_k \prod_{i \in P_k} p(C_k(i)|i) \quad (2)$$

Our inference strategy has two benefits: (a) Since the architecture is unchanged, the fully-connected layer can be run regularly (Table 5) or as decision rules (Table 1), and (b) unlike decision trees and

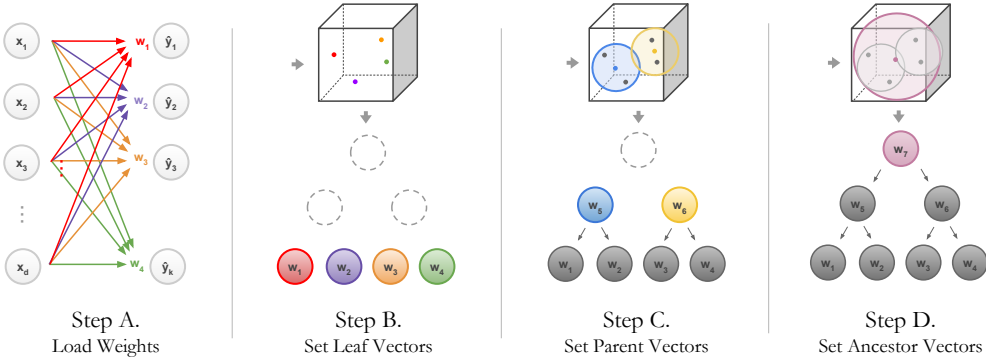


Figure 2: Building Induced Hierarchies. **Step A.** Load the weights of a pre-trained model’s final fully-connected layer, with weight matrix $W \in \mathbb{R}^{D \times K}$. **Step B.** Take rows $w_k \in W$ and normalize for each leaf node’s weight. For example, the red w_1 in A is assigned to the red leaf in B. **Step C.** Average each pair of leaf nodes for the parents’ weight. For example, w_1 and w_2 (red and purple) in B are averaged to make w_5 (blue) in C. **Step D.** For each ancestor, average all leaf node weights in its subtree. That average is the ancestor’s weight. Here, the ancestor is the root, so its weight is the average of all leaf weights w_1, w_2, w_3, w_4 .

other conditionally-executed models (Tanno et al., 2019; Veit & Belongie, 2018), our method can recover from a mistake early in the hierarchy with sufficient uncertainty in the incorrect path (Figure 1 C, Appendix Table 7). This inference mode bests classic tree inference (Appendix C.2).

3.2 BUILDING INDUCED HIERARCHIES

Existing decision-tree-based methods use (a) hierarchies built with data-dependent heuristics like information gain or (b) existing hierarchies like WordNet. However, the former overfits to the data, and the latter focuses on conceptual rather than visual similarity: For example, by virtue of being an animal, *Bird* is closer to *Cat* than to *Plane*, according to WordNet. However, the opposite is true for visual similarity: by virtue of being in the sky, *Bird* is more visually similar to *Plane* than to *Cat*. Thus, to prevent overfitting and reflect visual similarity, we build a hierarchy using model weights.

Our hierarchy requires pre-trained model weights. Take row vectors $w_k : k \in [1, K]$, each representing a class, from the fully-connected layer weights W . Then, run hierarchical agglomerative clustering on the normalized class representatives $w_k / \|w_k\|_2$. Agglomerative clustering decides which nodes and groups of nodes are iteratively paired. As described in Sec 3.1, each leaf node’s weight is a row vector $w_k \in W$ (Figure 2, Step B) and each inner node’s weight n_i is the average of its leaf node’s weights (Figure 2, Step C). This hierarchy is the *induced hierarchy* (Figure 2).

3.3 LABELING DECISION NODES WITH WORDNET

WordNet is a hierarchy of nouns. To assign WordNet meaning to nodes, we compute the earliest common ancestor for all leaves in a subtree: For example, say *Dog* and *Cat* are two leaves that share a parent. To find WordNet meaning for the parent, find all ancestor concepts that *Dog* and *Cat* share, like *Mammal*, *Animal*, and *Living Thing*. The earliest shared ancestor is *Mammal*, so we assign *Mammal* to the parent of *Dog* and *Cat*. We repeat for all inner nodes.

However, the WordNet corpus is lacking in concepts that are not themselves objects, like object attributes (e.g., *Pencil* and *Wire* are both cylindrical) and (b) abstract visual ideas like context (e.g., *fish* and *boat* are both aquatic). Many of these which are littered across our induced hierarchies (Appendix Figure 14). Despite this limitation, we use WordNet to assign meaning to intermediate decision nodes, with more sophisticated methods left to future work.

3.4 FINE-TUNING WITH TREE SUPERVISION LOSS

Even though standard cross entropy loss separates representatives for each leaf, it is not trained to separate representatives for each inner node (Table 3, “None”). To amend this, we add a *tree super-*

Table 1: Results. NBDT outperforms competing decision-tree-based methods by up to 18% and can also outperform the *original* neural network by $\sim 1\%$. “Expl?” indicates the method retains interpretable properties: pure leaves, sequential decisions, non-ensemble. Methods without this check see reduced interpretability. We bold the highest decision-tree-based accuracy. These results are taken directly from the original papers (*n/a* denotes results missing from original papers): XOC (Alaniz & Akata, 2019), DCDJ (Baek et al., 2017), NofE (Ahmed et al., 2016), DDN (Murthy et al., 2016), ANT (Tanno et al., 2019), CNN-RNN (Guo et al., 2018). We train DNDF (Kontschieder et al., 2015) with an updated R18 backbone, as they did not report CIFAR accuracy.

Method	Backbone	Expl?	CIFAR10	CIFAR100	TinyImageNet
NN	WideResNet28x10	✗	97.62%	82.09%	67.65%
ANT-A*	<i>n/a</i>	✓	93.28%	<i>n/a</i>	<i>n/a</i>
DDN	NiN	✗	90.32%	68.35%	<i>n/a</i>
DCDJ	NiN	✗	<i>n/a</i>	69.0%	<i>n/a</i>
NofE	ResNet56-4x	✗	<i>n/a</i>	76.24%	<i>n/a</i>
CNN-RNN	WideResNet28x10	✓	<i>n/a</i>	76.23%	<i>n/a</i>
NBDT-S (Ours)	WideResNet28x10	✓	97.55%	82.97%	67.72%
NN	ResNet18	✗	94.97%	75.92%	64.13%
DNDF	ResNet18	✗	94.32%	67.18%	44.56%
XOC	ResNet18	✓	93.12%	<i>n/a</i>	<i>n/a</i>
DT	ResNet18	✓	93.97%	64.45%	52.09%
NBDT-S (Ours)	ResNet18	✓	94.82%	77.09%	64.23%

vision loss, a cross entropy loss over the class distribution of path probabilities $\mathcal{D}_{\text{nbdt}} = \{p(k)\}_{k=1}^K$ (Eq. 1) from Sec 3.1, with time-varying weights ω_t, β_t where t is the epoch count:

$$\mathcal{L} = \beta_t \underbrace{\text{CROSSENTROPY}(\mathcal{D}_{\text{pred}}, \mathcal{D}_{\text{label}})}_{\mathcal{L}_{\text{original}}} + \omega_t \underbrace{\text{CROSSENTROPY}(\mathcal{D}_{\text{nbdt}}, \mathcal{D}_{\text{label}})}_{\mathcal{L}_{\text{soft}}} \quad (3)$$

Our tree supervision loss $\mathcal{L}_{\text{soft}}$ requires a pre-defined hierarchy. We find that (a) tree supervision loss damages learning speed early in training, when leaf weights are nonsensical. Thus, our tree supervision weight ω_t grows linearly from $\omega_0 = 0$ to $\omega_T = 0.5$ for CIFAR10, CIFAR100, and to $\omega_T = 5$ for TinyImageNet, ImageNet; $\beta_t \in [0, 1]$ decays linearly over time. (b) We re-train where possible, fine-tuning with $\mathcal{L}_{\text{soft}}$ only when the original model accuracy is not reproducible. (c) Unlike hierarchical softmax, our path-probability cross entropy loss $\mathcal{L}_{\text{soft}}$ disproportionately up-weights decisions earlier in the hierarchy, encouraging accurate high-level decisions; this is reflected our out-generalization of the baseline neural network by up to 16% to unseen classes (Table 6).

4 EXPERIMENTS

NBDTs obtain state-of-the-art results for interpretable models and match or outperform modern neural networks on image classification. We report results on different models (ResNet, WideResNet, EfficientNet) and datasets (CIFAR10, CIFAR100, TinyImageNet, ImageNet). We additionally conduct ablation studies to verify the hierarchy and loss designs, find that our training procedure improves the *original* neural network’s accuracy by up to 2%, and show that NBDTs improve generalization to unseen classes by up to 16%. All reported improvements are absolute.

4.1 RESULTS

Small-scale Datasets. Our method (Table 1) matches or outperforms recently state-of-the-art neural networks. On CIFAR10 and TinyImageNet, NBDT accuracy falls within 0.15% of the baseline neural network. On CIFAR100, NBDT accuracy outperforms the baseline by $\sim 1\%$.

Large-scale Dataset. On ImageNet (Table 3), NBDTs obtain 76.60% top-1 accuracy, outperforming the strongest competitor NofE by 15%. Note that we take the best competing results for any decision-tree-based method, but the strongest competitors hinder interpretability by using ensembles of models like a decision forest (DNDF, DCDJ) or feature shallow trees with only depth 2 (NofE).

Figure 3: ImageNet Results. NBDT outperforms all competing decision-tree-based methods by at least 14%, staying within 0.6% of EfficientNet accuracy. “EfficientNet” is EfficientNet-EdgeTPU-Small.

Method	NBDT (ours)	NBDT (ours)	XOC	NofE
Backbone	EfficientNet	ResNet18	ResNet152	AlexNet
Original Acc	77.23%	60.76%	78.31%	56.55%
Delta Acc	-0.63%	+0.50%	-17.5%	+4.7%
Explainable Acc	76.60%	61.26%	60.77%	61.29%

Table 2: Comparisons of Hierarchies. We demonstrate that our weight-space hierarchy bests taxonomy and data-dependent hierarchies. In particular, the induced hierarchy achieves better performance than (a) the WordNet hierarchy, (b) a classic decision tree’s information gain hierarchy, built over neural features (“Info Gain”), and (c) an oblique decision tree built over neural features (“OC1”).

Dataset	Backbone	Original	Induced	Info Gain	WordNet	OC1
CIFAR10	ResNet18	94.97%	94.82%	93.97%	94.37%	94.33%
CIFAR100	ResNet18	75.92%	77.09%	64.45%	74.08%	38.67%
TinyImageNet200	ResNet18	64.13%	64.23%	52.09%	60.26%	15.63%

4.2 ANALYSIS

Analyses show that our NBDT improvements are dominated by significantly improved ability to distinguish higher-level concepts (e.g., *Animal* vs. *Vehicle*).

Comparison of Hierarchies. Table 2 shows that our induced hierarchies outperform alternatives. In particular, *data-dependent* hierarchies overfit, and the existing *WordNet hierarchy* focuses on conceptual rather than visual similarity.

Comparisons of Losses. Previous work suggests hierarchical softmax (Appendix C.1) is necessary for hierarchical classifiers. However, our results suggest otherwise: NBDTs trained with hierarchical softmax see $\sim 3\%$ less accuracy than with tree supervision loss on TinyImageNet (Table 3).

Original Neural Network. Per Sec 3.1, we can run the original neural network’s fully-connected layer normally, after training with tree supervision loss. Using this, we find that the original neural network’s accuracy improves by up to 2% on CIFAR100, TinyImageNet (Table 5).

Zero-Shot Superclass Generalization. We define a “superclass” to be the hypernym of several classes. (e.g. *Animal* is a superclass of *Cat* and *Dog*). Using WordNet (per Sec 3.2), we (1) identify which superclasses each NBDT inner node is deciding between (e.g. *Animal* vs. *Vehicle*). (2) We find unseen classes that belong to the same superclass, from a different dataset. (e.g. Pull *Turtle* images from ImageNet). (3) Evaluate the model to ensure the unseen class is classified into the correct superclass (e.g. ensure *Turtle* is classified as *Animal*). For an NBDT, this is straightforward: one of the inner nodes classifies *Animal* vs. *Vehicle* (Sec 3.3). For a standard neural network, we consider the superclass that the final prediction belongs to. (*i.e.* When evaluating *Animal* vs. *Vehicle* on a *Turtle* image, the CIFAR-trained model may predict any CIFAR *Animal* class). See Appendix B.2 for details. Our NBDT consistently bests the original neural network by 8%+ (Table 6). When discerning *Carnivore* vs. *Ungulate*, NBDT outperforms the original neural network by 16%.

Mid-Training Hierarchy: We test NBDTs without using pre-trained weights, instead constructing hierarchies during training from the partially-trained network’s weights. Tree supervision loss with mid-training hierarchies reliably improve the original neural network’s accuracy, up to $\sim 0.6\%$, and the NBDT itself can match the original neural network’s accuracy (Table 4). However, this underperforms NBDT (Table 1), showing fully-trained weights are still preferred for hierarchy construction.

5 INTERPRETABILITY

By breaking complex decisions into smaller intermediate decisions, decision trees provide insight into the decision process. However, when the intermediate decisions are themselves neural network

Table 3: Comparisons of Losses. Training the NBDT using tree supervision loss with a linearly increasing weight (“TreeSup(t)”) is superior to training (a) with a constant-weight tree supervision loss (“TreeSup”), (b) with a hierarchical softmax (“HrchSmax”) and (c) without extra loss terms. (“None”). Δ is the accuracy difference between our soft loss and hierarchical softmax.

Dataset	Backbone	Original	TreeSup(t)	TreeSup	None	HrchSmax
CIFAR10	ResNet18	94.97%	94.82%	94.76%	94.38%	93.97%
CIFAR100	ResNet18	75.92%	77.09%	74.92%	61.93%	74.09%
TinyImageNet200	ResNet18	64.13%	64.23%	62.74%	45.51%	61.12%

Table 4: Mid-Training Hierarchy. Constructing and using hierarchies early and often in training yields the highest performing models. All experiments use ResNet18 backbones. Per Sec 3.4, β_t, ω_t are the loss term coefficients. Hierarchies are reconstructed every “Period” epochs, starting at “Start” and ending at “End”.

Hierarchy Updates			CIFAR10			CIFAR100		
Start	End	Period	NBDT	NN+TSL	NN	NBDT	NN+TSL	NN
67	120	10	94.88%	94.97%	94.97%	76.04%	76.56%	75.92%
90	140	10	94.29%	94.84%	94.97%	75.44%	76.29%	75.92%
90	140	20	94.52%	94.89%	94.97%	75.08%	76.11%	75.92%
120	121	10	94.52%	94.92%	94.97%	74.97%	75.88%	75.92%

predictions, extracting insight becomes more challenging. To address this, we adopt benchmarks and an interpretability definition offered by Poursabzi-Sangdeh et al. (2018): A model is interpretable if a human can validate its prediction, determining when the model has made a sizable mistake. To assess this, we adapt Poursabzi-Sangdeh et al. (2018)’s benchmarks to computer vision and show (a) humans can identify misclassifications with NBDT explanations more accurately than with saliency explanations (Sec 5.1), (b) a way to utilize NBDT’s entropy to identify ambiguous labels (Sec. 5.4), and (c) that humans prefer to agree with NBDT predictions when given a challenging image classification task (Sec. 5.2 & 5.3). Note that these analyses depend on three model properties that NBDT preserves: (1) discrete, sequential decisions, so that one path is selected; (2) pure leaves, so that one path picks one class; and (3) non-ensembled predictions, so that path to prediction attribution is discrete. In all surveys, we use CIFAR10-trained models with ResNet18 backbones.

5.1 SURVEY: IDENTIFYING FAULTY MODEL PREDICTIONS

In this section we aim to answer a question posed in (Poursabzi-Sangdeh et al., 2018) “*How well can someone detect when the model has made a sizable mistake?*”. In this survey, each user is given 3 images, 2 of which are correctly classified and 1 is mis-classified. Users must predict which image was incorrectly classified given a) the model explanations and b) *without* the final prediction. For saliency maps, this is a near-impossible task as saliency usually highlights the main object in the image, regardless of wrong or right. However, hierarchical methods provide a sensible sequence of

Table 5: Original Neural Network. We compare the model’s accuracy before and after the tree supervision loss, using ResNet18, WideResNet on CIFAR100, TinyImageNet. Our loss increases the original network accuracy consistently by $\sim .8 - 2.4\%$. NN-S is the network trained with the tree supervision loss.

Dataset	Backbone	NN	NN-S
C100	R18	75.92%	76.96%
T200	R18	64.13%	66.55%
C100	WRN28	82.09%	82.87%
T200	WRN28	67.65%	68.51%

Table 6: Zero-Shot Superclass Generalization. We evaluate a CIFAR10-trained NBDT (ResNet18 backbone) inner node’s ability to generalize beyond seen classes. We label TinyImageNet with superclass labels (e.g. label *Dog* with *Animal*) and evaluate nodes distinguishing between said superclasses. We compare to the baseline ResNet18: check if the prediction is within the right superclass.

n_{class}	Superclasses	R18	NBDT-S
71	Animal vs. Vehicle	66.08%	74.79%
36	Placental vs. Vertebrate	45.50%	54.89%
19	Carnivore vs. Ungulate	51.37%	67.78%
9	Motor Vehicle vs. Craft	69.33%	77.78%

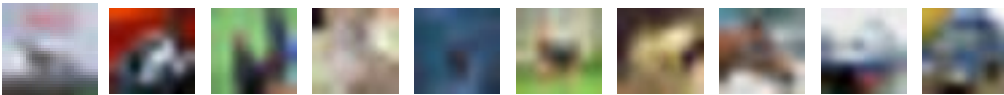


Figure 4: CIFAR10 Blurry Images. To make the classification task difficult for humans, the CIFAR10 images are downsampled by $4\times$. This forces at least partial reliance on model predictions, allowing us to evaluate which explanations are convincing enough to earn the user’s agreement.

intermediate decisions that can be checked. This is reflected in the results: For each explainability technique, we collected **600** survey responses. When given saliency maps and class probabilities, only **87** predictions were correctly identified as wrong. In comparison, when given the NBDT series of predicted classes and child probabilities (e.g., “Animal (90%) → Mammal (95%)”, without the final leaf prediction) **237** images were correctly identified as wrong. Thus, respondents can better recognize mistakes in NBDT explanations nearly 3 times better.

Although NBDT provides more information than saliency maps about misclassification, a majority – the remaining 363 NBDT predictions – were not correctly identified. To explain this, we note that $\sim 37\%$ of all NBDT errors occur at the final binary decision, between two leaves; since we provide all decisions except the final one, these leaf errors would be impossible to distinguish.

5.2 SURVEY: EXPLANATION-GUIDED IMAGE CLASSIFICATION

In this section we aim to answer a question posed in (Poursabzi-Sangdeh et al., 2018) “*To what extent do people follow a model’s predictions when it is beneficial to do so?*”. In this first survey, each user is asked to classify a severely blurred image (Fig 4). This survey affirms the problem’s difficulty, decimating human performance to not much more than guessing: **163** of **600** responses are correct (27.2% accuracy).

In the next survey, we offer the blurred image and two sets of predictions: (1) the original neural network’s predicted class and its saliency map, and (2) the NBDT predicted class and the sequence of decisions that led up to it (“Animal, Mammal, Cat”). For all examples, the two models predict different classes. In 30% of the examples, NBDT is right and the original model is wrong. In another 30%, the opposite is true. In the last 40%, both models are wrong. As shown in Fig. 4, the image is extremely blurry, so the user must rely on the models to inform their prediction. When offered model predictions, in this survey, **255** of **600** responses are correct (42.5% accuracy), a 15.3 point improvement over no model guidance. We observe that humans trust NBDT-explained prediction more often than the saliency-explained predictions. Out of **600** responses, **312** responses agreed with the NBDT’s prediction, **167** responses agreed with the base model’s prediction, and **119** responses disagreed with both model’s predictions. Note that a majority of user decisions ($\sim 80\%$) agreed with either model prediction, even though neither model prediction was correct in 40% of examples, showing our images were sufficiently blurred to force reliance on the models. Furthermore, 52% of responses agreed with NBDT (against saliency’s 28%), even though only 30% of NBDT predictions were correct, showing improvement in model trust.

5.3 SURVEY: HUMAN-DIAGNOSED LEVEL OF TRUST

The explanation of an NBDT prediction is the visualization of the path traversed. We then compare these NBDT explanations to other explainability methods in human studies. Specifically, we ask participants to pick an expert to trust (Appendix, Figure 13), based on the expert’s explanation – a saliency map (ResNet18, GradCAM), a decision tree (NBDT), or neither. We only use samples where ResNet18 and NBDT predictions agree. Of 374 respondents that picked one method over the other, **65.9%** prefer NBDT explanations; for misclassified samples, **73.5%** prefer NBDT. This supports the previous survey’s results, showing humans trust NBDTs more than current saliency techniques when explicitly asked.

5.4 ANALYSIS: IDENTIFYING FAULTY DATASET LABELS

There are several types of ambiguous labels (Figure 5), any of which could hurt model performance for an image classification dataset like ImageNet. To find these images, we use entropy in NBDT

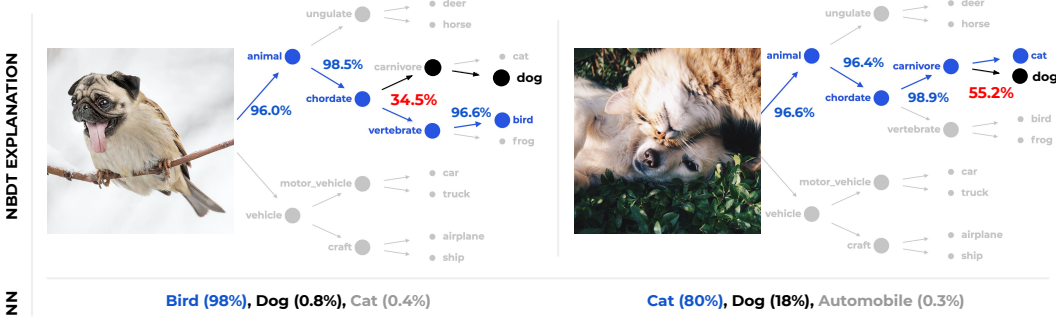


Figure 5: Types of Ambiguous Labels. All these examples have ambiguous labels. With NBDT (top), the decision rule deciding between equally-plausible classes has low certainty (red, 30-50%). All other decision rules have high certainty (blue, 96%+). The juxtaposition of high and low certainty decision rules makes ambiguous labels easy to distinguish. By contrast, ResNet18 (bottom) still picks one class with high probability. (Left) An extreme example of a “spug” that may plausibly belong to two classes. (Right) Image containing two animals of different classes. Photo ownership: “Spug” by Arne Fredriksen at gyporrama.com. Used with permission. Second image is CC-0 licensed at pexels.com.

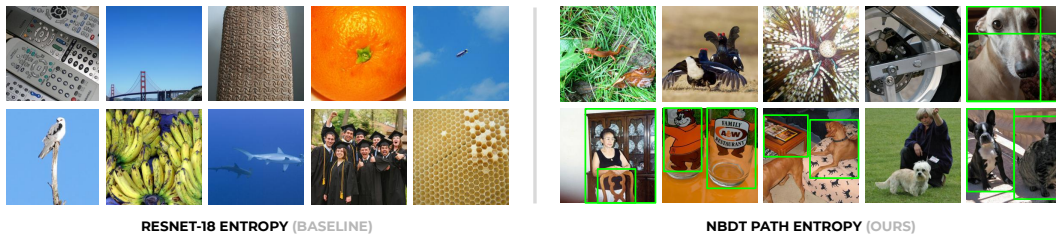


Figure 6: ImageNet Ambiguous Labels. These images suggest that NBDT path entropy uniquely identifies ambiguous labels in Imagenet, without object detection labels. We plot ImageNet validation samples that induce the most 2-class confusion, using TinyImagenet200-trained models. Note that ImageNet classes do not include people. (Left) Run ResNet18 and find samples that (a) maximize entropy between the top 2 classes and (b) minimize entropy across all classes, where the top 2 classes are averaged. Despite high model uncertainty, half the classes are from the training set – bee, orange, bridge, banana, remote control – and do not show visual ambiguity. (Right) For NBDT, compute entropy for each node’s predicted distribution; take the difference between the largest and smallest values. Now, half of the images contain truly ambiguous content for a classifier; we draw green boxes around pairs of objects that could each plausibly be used for the image class.

decisions, which we find is a much stronger indicator of ambiguity than entropy in the original neural network prediction. The intuition is as follows: If all intermediate decisions have high certainty except for a few decisions, those decisions are deciding between multiple equally plausible cases. Using this intuition, we can identify ambiguous labels by finding samples with high “path entropy” – or highly disparate entropies for intermediate decisions on the NBDT prediction path.

Per Figure 6, the highest “path entropy” samples in ImageNet contain multiple objects, where each object could plausibly be used for the image class. In contrast, samples that induce the highest entropy in the baseline neural network do not suggest ambiguous labels. This suggests NBDT entropy is more informative compared to that of a standard neural network.

6 CONCLUSION

In this work, we propose Neural-Backed Decision Trees that see (1) improved accuracy: NBDTs out-generalize (16%+), improve (2%+), and match (0.15%) or outperform (1%+) state-of-the-art neural networks on CIFAR10, CIFAR100, TinyImageNet, and ImageNet. We also show (2) improved interpretability by drawing unique insights from our hierarchy, confirming that humans trust NBDT’s over saliency and illustrate how path entropy can be used to identify ambiguous labels. This challenges the conventional supposition of a dichotomy between accuracy and interpretability, paving the way for jointly accurate *and* interpretable models in real-world deployments.

REFERENCES

- Karim Ahmed, Mohammadharis Baig, and Lorenzo Torresani. Network of experts for large-scale image categorization. volume 9911, April 2016.
- Stephan Alaniz and Zeynep Akata. XOC: explainable observer-classifier for explainable binary decisions. *CoRR*, abs/1902.01780, 2019.
- Seungryul Baek, Kwang In Kim, and Tae-Kyun Kim. Deep convolutional decision jungle for image classification. *CoRR*, abs/1706.02003, 2017.
- Arunava Banerjee. Initializing neural networks using decision trees. 1990.
- Arunava Banerjee. Initializing neural networks using decision trees. In *Proceedings of the International Workshop on Computational Learning and Natural Learning Systems*, pp. 3–15. MIT Press, 1994.
- Ufuk Can Biçici, Cem Keskin, and Lale Akarun. Conditional information gain networks. In *2018 24th International Conference on Pattern Recognition (ICPR)*, pp. 1390–1395. IEEE, 2018.
- Olcay Boz. Converting a trained neural network to a decision tree dectext - decision tree extractor. In *ICMLA*, 2000.
- Clemens-Alexander Brust and Joachim Denzler. Integrating domain knowledge: using hierarchies to improve deep classifiers. In *Asian Conference on Pattern Recognition*, pp. 3–16. Springer, 2019.
- Diogo V Carvalho, Eduardo M Pereira, and Jaime S Cardoso. Machine learning interpretability: A survey on methods and metrics. *Electronics*, 8(8):832, 2019.
- Mark Craven and Jude W Shavlik. Extracting tree-structured representations of trained networks. In *Advances in neural information processing systems*, pp. 24–30, 1996.
- Mark W Craven and Jude W Shavlik. Using sampling and queries to extract rules from trained neural networks. In *Machine learning proceedings 1994*, pp. 37–45. Elsevier, 1994.
- Darren Dancey, David McLean, and Zuhair Bandar. Decision tree extraction from trained neural networks. January 2004.
- J. Deng, W. Dong, R. Socher, L.-J. Li, K. Li, and L. Fei-Fei. ImageNet: A Large-Scale Hierarchical Image Database. In *CVPR09*, 2009.
- Jia Deng, Nan Ding, Yangqing Jia, Andrea Frome, Kevin Murphy, Samy Bengio, Yuan Li, Hartmut Neven, and Hartwig Adam. Large-scale object classification using label relation graphs.
- Jia Deng, Jonathan Krause, Alexander C Berg, and Li Fei-Fei. Hedging your bets: Optimizing accuracy-specificity trade-offs in large scale visual recognition. In *2012 IEEE Conference on Computer Vision and Pattern Recognition*, pp. 3450–3457. IEEE, 2012.
- Finale Doshi-Velez and Been Kim. Towards a rigorous science of interpretable machine learning. *arXiv preprint arXiv:1702.08608*, 2017.
- Dheeru Dua and Casey Graff. UCI machine learning repository, 2017. URL <http://archive.ics.uci.edu/ml>.
- Nicholas Frosst and Geoffrey E. Hinton. Distilling a neural network into a soft decision tree. *CoRR*, abs/1711.09784, 2017.
- Yanming Guo, Yu Liu, Erwin M Bakker, Yuanhao Guo, and Michael S Lew. Cnn-rnn: a large-scale hierarchical image classification framework. *Multimedia Tools and Applications*, 77(8):10251–10271, 2018.
- Geoffrey Hinton, Oriol Vinyals, and Jeff Dean. Distilling the knowledge in a neural network. *arXiv preprint arXiv:1503.02531*, 2015.

- Kelli Humbird, Luc Peterson, and Ryan McClaren. Deep neural network initialization with decision trees. *IEEE Transactions on Neural Networks and Learning Systems*, PP:1–10, October 2018.
- Irena Ivanova and Miroslav Kubat. Initialization of neural networks by means of decision trees. *Knowledge-Based Systems*, 8(6):333 – 344, 1995a. Knowledge-based neural networks.
- Irena Ivanova and Miroslav Kubat. Decision-tree based neural network (extended abstract). In *Machine Learning: ECML-95*, pp. 295–298, Berlin, Heidelberg, 1995b. Springer Berlin Heidelberg.
- Cem Keskin and Shahram Izadi. Splinenets: Continuous neural decision graphs. In *Advances in Neural Information Processing Systems*, pp. 1994–2004, 2018.
- Peter Kotschieder, Madalina Fiterau, Antonio Criminisi, and Samuel Rota Bulo. Deep neural decision forests. In *The IEEE International Conference on Computer Vision (ICCV)*, December 2015.
- R. Krishnan, G. Sivakumar, and P. Bhattacharya. Extracting decision trees from trained neural networks. *Pattern Recognition*, 32(12):1999 – 2009, 1999.
- Alex Krizhevsky. Learning multiple layers of features from tiny images. Technical report, 2009.
- Ya Le and Xuan Yang. Tiny imagenet visual recognition challenge. 2015.
- Yann LeCun, Corinna Cortes, and CJ Burges. Mnist handwritten digit database. *ATT Labs [Online]*. Available: <http://yann.lecun.com/exdb/mnist>, 2, 2010.
- Zachary Chase Lipton. The mythos of model interpretability. corr abs/1606.03490 (2016). *arXiv preprint arXiv:1606.03490*, 2016.
- SM Lundberg, G Erion, H Chen, A DeGrave, JM Prutkin, B Nair, R Katz, J Himmelfarb, N Bansal, and S-i Lee. From local explanations to global understanding with explainable ai for trees, nat. mach. intell., 2, 56–67, 2020.
- Mason McGill and Pietro Perona. Deciding how to decide: Dynamic routing in artificial neural networks. In *ICML*, 2017.
- Abdul Arfat Mohammed and Venkatesh Umaashankar. Effectiveness of hierarchical softmax in large scale classification tasks. In *2018 International Conference on Advances in Computing, Communications and Informatics (ICACCI)*, pp. 1090–1094. IEEE, 2018.
- Calvin Murdock, Zhen Li, Howard Zhou, and Tom Duerig. Blockout: Dynamic model selection for hierarchical deep networks. In *Proceedings of the IEEE conference on computer vision and pattern recognition*, pp. 2583–2591, 2016.
- Venkatesh N. Murthy, Vivek Singh, Terrence Chen, R. Manmatha, and Dorin Comaniciu. Deep decision network for multi-class image classification. In *The IEEE Conference on Computer Vision and Pattern Recognition (CVPR)*, June 2016.
- Vitali Petsiuk, Abir Das, and Kate Saenko. Rise: Randomized input sampling for explanation of black-box models. In *Proceedings of the British Machine Vision Conference (BMVC)*, 2018.
- F Poursabzi-Sangdeh, D Goldstein, J Hofman, J Vaughan, and H Wallach. Manipulating and measuring model interpretability. In *MLConf*, 2018.
- Joseph Redmon and Ali Farhadi. Yolo9000: better, faster, stronger. In *Proceedings of the IEEE conference on computer vision and pattern recognition*, pp. 7263–7271, 2017.
- Marco Tulio Ribeiro, Sameer Singh, and Carlos Guestrin. ”why should I trust you?”: Explaining the predictions of any classifier. In *Proceedings of the 22nd ACM SIGKDD International Conference on Knowledge Discovery and Data Mining, San Francisco, CA, USA, August 13-17, 2016*, pp. 1135–1144, 2016.
- Samuel Rota Bulo and Peter Kotschieder. Neural decision forests for semantic image labelling. In *Proceedings of the IEEE Conference on Computer Vision and Pattern Recognition*, pp. 81–88, 2014.

- Anirban Roy and Sinisa Todorovic. Monocular depth estimation using neural regression forest. In *Proceedings of the IEEE conference on computer vision and pattern recognition*, pp. 5506–5514, 2016.
- C Rudin. Stop explaining black box machine learning models for high stakes decisions and use interpretable models instead. manuscript based on c. rudin please stop explaining black box machine learning models for high stakes decisions. In *Proceedings of NeurIPS 2018 Workshop on Critiquing and Correcting Trends in Learning*, 2018.
- Ramprasaath R Selvaraju, Michael Cogswell, Abhishek Das, Ramakrishna Vedantam, Devi Parikh, and Dhruv Batra. Grad-cam: Visual explanations from deep networks via gradient-based localization. In *IEEE Conference on Computer Vision and Pattern Recognition (CVPR)*, pp. 618–626, 2017.
- Noam Shazeer, Azalia Mirhoseini, Krzysztof Maziarz, Andy Davis, Quoc Le, Geoffrey Hinton, and Jeff Dean. Outrageously large neural networks: The sparsely-gated mixture-of-experts layer. *arXiv preprint arXiv:1701.06538*, 2017.
- Carlos N Silla and Alex A Freitas. A survey of hierarchical classification across different application domains. *Data Mining and Knowledge Discovery*, 22(1-2):31–72, 2011.
- Karen Simonyan, Andrea Vedaldi, and Andrew Zisserman. Deep inside convolutional networks: Visualising image classification models and saliency maps. *arXiv preprint arXiv:1312.6034*, 2013.
- Chapman Siu. Transferring tree ensembles to neural networks. In *Neural Information Processing*, pp. 471–480, 2019.
- Jost Tobias Springenberg, Alexey Dosovitskiy, Thomas Brox, and Martin A. Riedmiller. Striving for simplicity: The all convolutional net. *CorR*, abs/1412.6806, 2014.
- Mukund Sundararajan, Ankur Taly, and Qiqi Yan. Axiomatic attribution for deep networks. *International Conference on Machine Learning (ICML) 2017*, 2017.
- Ryutaro Tanno, Kai Arulkumaran, Daniel C. Alexander, Antonio Criminisi, and Aditya Nori. Adaptive neural trees, 2019.
- Ravi Teja Mullapudi, William R. Mark, Noam Shazeer, and Kayvon Fatahalian. Hydranets: Specialized dynamic architectures for efficient inference. In *The IEEE Conference on Computer Vision and Pattern Recognition (CVPR)*, June 2018.
- Andreas Veit and Serge Belongie. Convolutional networks with adaptive inference graphs. In *The European Conference on Computer Vision (ECCV)*, September 2018.
- Mike Wu, M Hughes, Sonali Parbhoo, and F Doshi-Velez. Beyond sparsity: Tree-based regularization of deep models for interpretability. In *In: Neural Information Processing Systems (NIPS) Conference. Transparent and Interpretable Machine Learning in Safety Critical Environments (TIML) Workshop*, 2017.
- Brandon Yang, Gabriel Bender, Quoc V Le, and Jiquan Ngiam. Condconv: Conditionally parameterized convolutions for efficient inference. In *Advances in Neural Information Processing Systems*, pp. 1307–1318, 2019.
- Matthew D Zeiler and Rob Fergus. Visualizing and understanding convolutional networks. In *European Conference on Computer Vision (ECCV)*, pp. 818–833. Springer, 2014.
- Jianming Zhang, Zhe Lin, Jonathan Brandt, Xiaohui Shen, and Stan Sclaroff. Top-down neural attention by excitation backprop. In *European Conference on Computer Vision (ECCV)*, pp. 543–559. Springer, 2016.

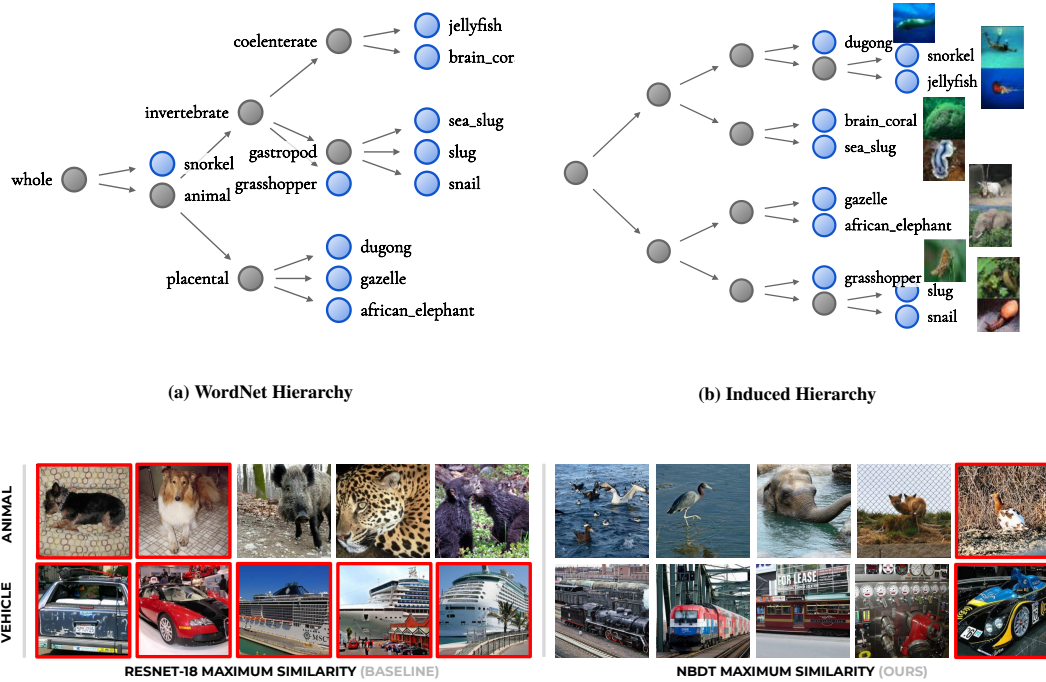


Figure 8: Maximum Similarity Examples. We run two CIFAR10-trained models, one trained with tree supervision loss (NBDT) and one without tree supervision loss (ResNet18). We compute the induced hierarchy of both models and find samples most similar to the *Animal*, and *Motor Vehicle* concepts. Each row represents an inner node, and the red borders indicate images that contain CIFAR10 classes. (1) Note that NBDT’s concept of an animal includes classes and contexts it was not trained on; aquatic animals (top-right) and trains (bottom-right) are not a part of CIFAR10. In contrast, ResNet18 largely finds examples closely related to existing CIFAR10 classes (dog, car, boat). This is qualitative evidence that NBDTs better generalize.

A ACKNOWLEDGMENTS

In addition to NSF CISE Expeditions Award CCF-1730628, UC Berkeley research is supported by gifts from Alibaba, Amazon Web Services, Ant Financial, CapitalOne, Ericsson, Facebook, Futurewei, Google, Intel, Microsoft, Nvidia, Scotiabank, Splunk and VMware. This material is based upon work supported by the National Science Foundation Graduate Research Fellowship under Grant No. DGE 1752814.

B EXPLAINABILITY

In this section, we expand on details for interpretability as presented in the original paper, with an emphasis on qualitative use of the hierarchy.

B.1 MAXIMUM SIMILARITY EXAMPLES TO VISUALIZE GENERALIZATION

We (1) visually confirm the hypothesized meaning of each node by identifying the most “representative” samples, and (2) check that these “representative” samples represent that category (e.g., *Animal*) and not just the training classes under that category. We define “representative” samples, or maximum similarity examples, to be samples with embeddings most similar to an inner node’s representative. We visualize these examples for a model before and after the tree supervision loss (NBDT and ResNet18, respectively). The models are trained on CIFAR10, but samples are drawn from ImageNet. We observe that maximum similarity examples for NBDT contain more unseen classes than ResNet18 (Figure 8). This suggests that our NBDT is better able to capture high-level concepts such as *Animal*, which is quantitatively confirmed by the superclass evaluation in Table 6.

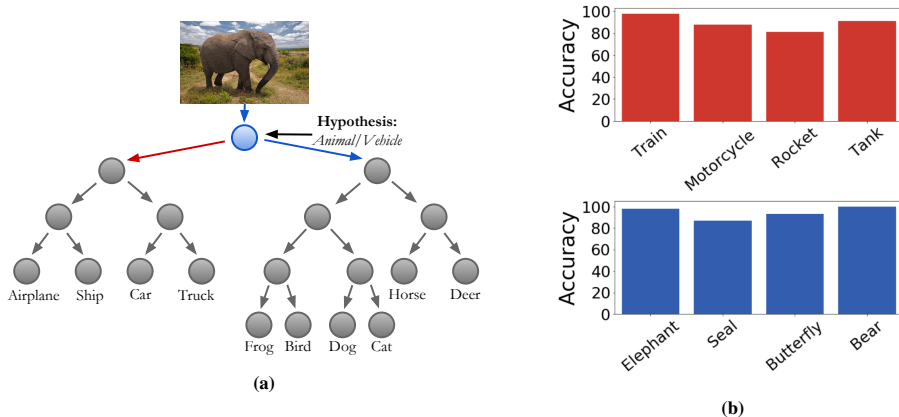


Figure 9: A Node’s meaning. (Left) Visualization of node hypothesis test performed on a CIFAR10-trained WideResNet28x10 model, by sampling from CIFAR100 validation set for OOD classes. (Right) Classification accuracy is high (80-95%) given unseen CIFAR100 samples of *Vehicles* (top) and *Animals* (bottom), for the WordNet-hypothesized *Animal/Vehicle* node.

B.2 EXPLAINABILITY OF NODES’ VISUAL MEANINGS

This section describes the method used in Table 6 in more detail. Since the induced hierarchy is constructed using model weights, the intermediate nodes are not forced to split on foreground objects. While hierarchies like WordNet provide hypotheses for a node’s meaning, the tree may split on unexpected contextual and visual attributes such as *underwater* and *on land*, depicted in Figure 7b. To diagnose a node’s visual meaning, we perform the following 4-step test:

1. Posit a hypothesis for the node’s meaning (e.g. *Animal vs. Vehicle*). This hypothesis can be computed automatically from a given taxonomy or deduced from manual inspection of each child’s leaves (Figure 9).
2. Collect a dataset with new, unseen classes that test the hypothesised meaning from step 1 (e.g. *Elephant* is an unseen *Animal*). Samples in this dataset are referred to as out-of-distribution (OOD) samples, as they are drawn from a separate labeled dataset.
3. Pass samples from this dataset through the node. For each sample, check whether the selected child node agrees with the hypothesis.
4. The accuracy of the hypothesis is the percentage of samples passed to the correct child. If the accuracy is low, repeat with a different hypothesis.

Figure 9a depicts the CIFAR10 tree induced by a WideResNet28x10 model trained on CIFAR10. The WordNet hypothesis is that the root note splits on *Animal vs. Vehicle*. We use the CIFAR100 validation set as out-of-distribution images for *Animal* and *Vehicle* classes that are unseen at training time. We then compute the hypothesis’ accuracy. Figure 9b shows our hypothesis accurately predicts which child each unseen-class’s samples traverse.

B.3 HOW MODEL ACCURACY AFFECTS INTERPRETABILITY

Induced hierarchies are determined by the proximity of class weights, but classes that are close in weight space may not have similar visual meaning: Figure 10 depicts the trees induced by WideResNet28x10 and ResNet10, respectively. While the WideResNet induced hierarchy (Figure 10a) groups visually-similar classes, the ResNet (Figure 10b) induced hierarchy does not, grouping classes such as *Frog*, *Cat*, and *Airplane*. This disparity in visual meaning is explained by WideResNet’s 4% higher accuracy: we believe that higher-accuracy models exhibit more visually-sound weight spaces. Thus, unlike previous work, NBDTs feature better interpretability with higher accuracy, instead of sacrificing one for the other. Furthermore, the disparity in hierarchies indicates that a model with low accuracy will not provide interpretable insight into high-accuracy decisions.

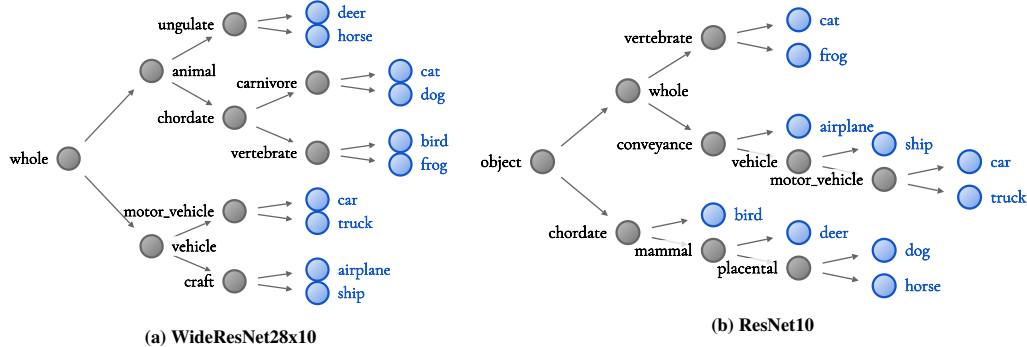


Figure 10: CIFAR10 induced hierarchies, with automatically-generated WordNet hypotheses for each node. The higher-accuracy (a) WideResNet (97.62% acc) has a more sensible hierarchy than (b) ResNet’s (93.64% acc): The former groups all *Animals* together, separate from all *Vehicles*. By contrast, the latter groups *Airplane*, *Cat*, and *Frog*.

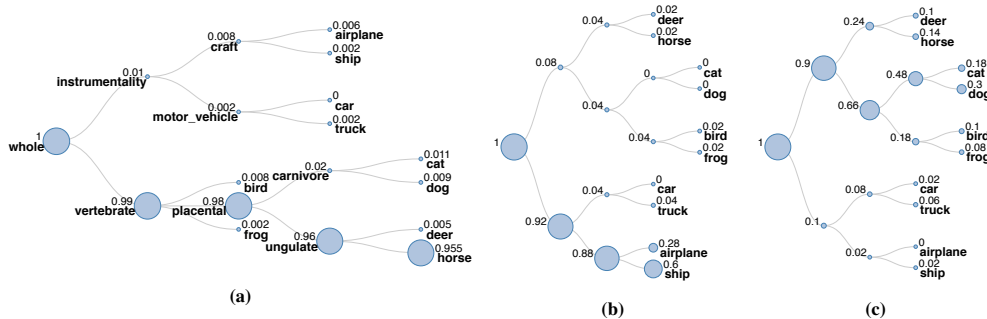


Figure 11: Visualization of path traversal frequency on an induced hierarchy for CIFAR10. (a) **In-Distribution:** *Horse* is a training class and thus sees highly focused path traversals. (b) **Unseen Class:** *Seashore* is largely classified as *Ship* despite not containing any objects, exhibiting model reliance on context (water). (c) **Unseen Class:** *Teddy Bear* is classified as *Dog*, for sharing visual attributes like color and texture.

B.4 VISUALIZATION OF TREE TRAVERSAL

Frequency of path traversals additionally provide insight into general model behavior. Figure 11 shows frequency of path traversals for all samples in three classes: a seen class, an unseen class but with seen context, and an unseen class with unseen context.

Seen class, seen context: We visualize tree traversals for all samples in CIFAR10’s *Horse* class (Figure 11a). As this class is present during training, tree traversal highlights the correct path with extremely high frequency. **Unseen class, seen context:** In Figure 11b, we visualize tree traversals for TinyImagenet’s *Seashore* class. The model classifies 88% of *Seashore* samples as “vehicle with blue context,” exhibiting reliance on context for decision-making. **Unseen class, unseen context:** In Figure 11c, we visualize traversals for TinyImagenet’s *Teddy Bear*. The model classifies 90% as *Animal*, belying the model’s generalization to stuffed animals. However, the model disperses samples among animals more evenly, with the most furry animal *Dog* receiving the most *Teddy Bear* samples (30%).

C HIERARCHICAL SOFTMAX AND CONDITIONAL EXECUTION

In the context of neural network and decision tree hybrids, many works (Shazeer et al., 2017; Keskin & Izadi, 2018; Yang et al., 2019; Tanno et al., 2019) leverage conditional execution to improve computational efficiency in a hierarchical classifier. One motivation is to handle large-scale classification problems.

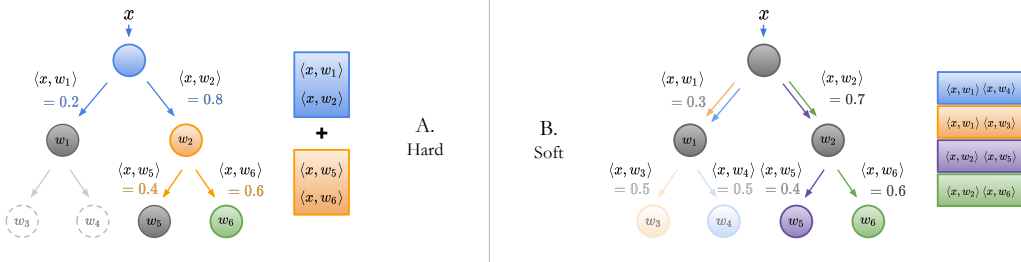


Figure 12: Tree Supervision Loss has two variants: **Hard Tree Supervision Loss (A)** defines a cross entropy term per node. This is illustrated with the blue box for the blue node and the orange box for the orange node. The cross entropy is taken over the child node probabilities. The green node is the leaf representing a class label. The dotted nodes are not included in the path from the label to the root, so do not have a defined loss. **Soft Tree Supervision Loss (B)** defines a cross entropy loss over all leaf probabilities. The probability of the green leaf is the product of the probabilities leading up to the root (in this case, $\langle x, w_2 \rangle \langle x, w_6 \rangle = 0.6 \times 0.7$). The probabilities for the other leaves are similarly defined. Each leaf probability is represented with a colored box. The cross entropy is then computed over this leaf probability distribution, represented by the colored box stacked on one another.

C.1 HARD TREE SUPERVISION LOSS

An alternative loss would be hierarchical softmax – in other words, one cross entropy loss per decision rule. We denote this the *hard tree supervision loss*, as we construct a variant of hierarchical softmax that (a) supports arbitrary depth trees and (b) is defined over a single, un-augmented fully-connected layer (e.g. k -dimensional output for a k -leaf tree). The original neural network’s loss $\mathcal{L}_{\text{original}}$ minimizes cross entropy across the classes. For a k -class dataset, this is a k -way cross entropy loss. Each internal node’s goal is similar: minimize cross-entropy loss across the child nodes. For node i with c children, this is a c -way cross entropy loss between predicted probabilities $\mathcal{D}(i)_{\text{pred}}$ and labels $\mathcal{D}(i)_{\text{label}}$. We refer to this collection of new loss terms as the *hard tree supervision loss* (Eq. 4). The individual cross entropy losses for each node are scaled so that the original cross entropy loss and the tree supervision loss are weighted equally, by default. If we assume N nodes in the tree, excluding leaves, then we would have $N + 1$ different cross entropy loss terms – the original cross entropy loss and N hard tree supervision loss terms. This is $\mathcal{L}_{\text{original}} + \mathcal{L}_{\text{hard}}$, where:

$$\mathcal{L}_{\text{hard}} = \frac{1}{N} \sum_{i=1}^N \underbrace{\text{CROSSENTROPY}(\mathcal{D}(i)_{\text{pred}}, \mathcal{D}(i)_{\text{label}})}_{\text{over the } c \text{ children for each node}}. \quad (4)$$

C.2 HARD INFERENCE

Hard inference is more intuitive: Starting at the root node, each sample is sent to the child with the most similar representative. We continue picking and traversing the tree until we reach a leaf. The class associated with this leaf is our prediction (Figure 1, A. Hard). More precisely, consider a tree with nodes indexed by i with set of child nodes $C(i)$. Each node i produces a probability of child node $j \in C(i)$; this probability is denoted $p(j|i)$. Each node thus picks the next node using $\text{argmax}_{j \in C(i)} p(j|i)$.

Whereas this inference mode is more intuitive, it underperforms soft inference (Figure 7). Furthermore, note that hard tree supervision loss (*i.e.* modified hierarchical softmax) appears to more specifically optimize hard inference. Despite that, hard inference performs worse (Figure 8) with hard tree supervision loss than the “soft” tree supervision loss (Sec 3.4) used in the main paper.

D IMPLEMENTATION

Our inference strategy, as outlined above and in Sec. 3.1 of the paper, includes two phases: (1) featurizing the sample using the neural network backbone and (2) running the embedded decision rules. However, in practice, our inference implementation does not need to run inference with the

Table 7: Comparisons of Inference Modes Hard inference performs worse than soft inference. See Table 1 in the main manuscript for a comparison against baselines.

Method	Backbone	CIFAR10	CIFAR100	TinyImageNet
NN	WideResNet28x10	97.62%	82.09%	67.65%
NBDT-H (Ours)	WideResNet28x10	97.55%	82.21%	64.39%
NBDT-S (Ours)	WideResNet28x10	97.55%	82.97%	67.72%
NN	ResNet18	94.97%	75.92%	64.13%
NBDT-H (Ours)	ResNet18	94.50%	74.29%	61.60%
NBDT-S (Ours)	ResNet18	94.82%	77.09%	63.77%

Table 8: Tree Supervision Loss Training the NBDT with the tree supervision loss (“TSL”) is superior to (a) training with a hierarchical softmax (“HS”) and to (b) omitting extra loss terms. (“None”). Δ is the accuracy difference between our soft loss and hierarchical softmax.

Dataset	Backbone	NN	Inference	None	TSL	HS	Δ
CIFAR10	ResNet18	94.97%	Hard	94.32%	94.50%	93.94%	+0.56%
CIFAR10	ResNet18	94.97%	Soft	94.38%	94.82%	93.97%	+0.85%
CIFAR100	ResNet18	75.92%	Hard	57.63%	74.29%	73.23%	+0.94%
CIFAR100	ResNet18	75.92%	Soft	61.93%	77.09%	74.09%	+1.83%
TinyImageNet	ResNet18	64.13%	Hard	39.57%	61.60%	58.89%	+2.71%
TinyImageNet	ResNet18	64.13%	Soft	45.51%	63.77%	61.12%	+2.65%

backbone, separately. In fact, our inference implementation only requires the logits \hat{y} outputted by the network. This is motivated by the knowledge that the average of inner products is equivalent to the inner product of averages. Knowing this, we have the following equivalence, given the fully-connected layer weight matrix W , its row vectors w_i , featurized sample x , and the classes C we are currently interested in.

$$\langle x, \frac{1}{n} \sum_{i=1}^{|C|} w_i \rangle = \frac{1}{n} \sum_{i=1}^{|C|} \langle x, w_i \rangle = \frac{1}{n} \sum_{i=1}^{|C|} \hat{y}_i, i \in C \quad (5)$$

Thus, our inference implementation is simply performed using the logits \hat{y} output by the network.

E EXPERIMENTAL SETUP

To reiterate, our best-performing models for both hard and soft inference were obtained by training with the soft tree supervision loss. All CIFAR10 and CIFAR100 experiments weight the soft loss terms by 1. All TinyImagenet and Imagenet experiments weight the soft loss terms by 10. We found that hard loss performed best when the hard loss weight was $10\times$ that of the corresponding soft loss weight (e.g. weight 10 for CIFAR10, CIFAR100; and weight 100 for TinyImagenet, Imagenet); these hyper-parameters are use for the tree supervision loss comparisons in Table 3.

Where possible, we retrain the network from scratch with tree supervision loss. For our remaining training hyperparameters, we largely use default settings found in github.com/kuangliu/pytorch-cifar: SGD with 0.9 momentum, 5^{-4} weight decay, a starting learning rate of 0.1, decaying by 90% $\frac{3}{7}$ and $\frac{5}{7}$ of the way through training. We make a few modifications: Training lasts for 200 epochs instead of 350, and we use batch sizes of 512 and 128 on one Titan Xp for CIFAR and TinyImagenet respectively.

In cases where we were unable to reproduce the baseline accuracy (WideResNet), we fine-tuned a pretrained checkpoint with the same settings as above, except with starting learning rate of 0.01.

On Imagenet, we retrain the network from scratch with tree supervision loss. For our remaining hyperparameters, we use settings reported to reproduce EfficientNet-EdgeTPU-Small results at github.com/rwrightman/pytorch-image-models: batch size 128, RMSProp with start-

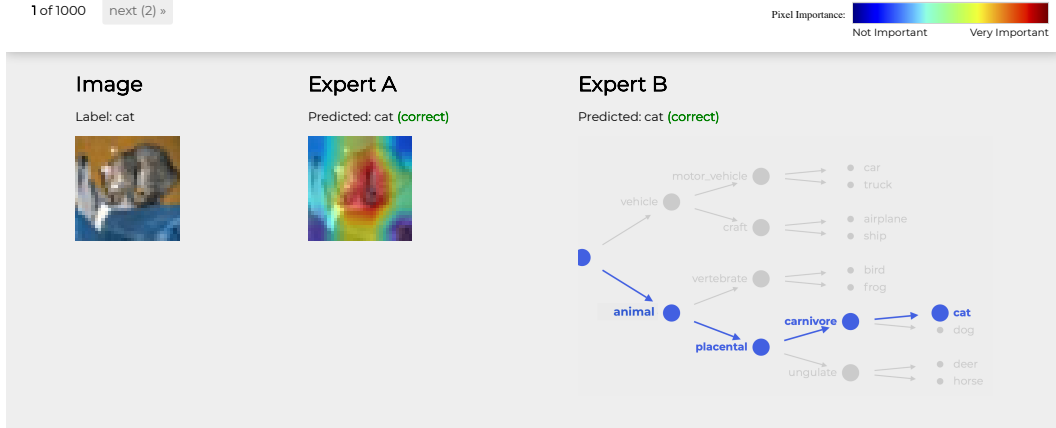


Figure 13: An example of a survey question presented to mechanical turks.

ing learning rate of 0.064, decaying learning rate by 97% every 2.4 epochs, weight decay of 10^{-5} , drop-connect with probability 0.2 on 8 V100s. Our results were obtained with only one model, as opposed to averaging over 8 models, so our reported baseline is 77.23%, as reported by the EfficientNet authors: <https://github.com/tensorflow/tpu/tree/master/models/official/efficientnet/edgetpu#post-training-quantization>.

F CIFAR10 TREE VISUALIZATION

We presented the tree visualizations for various models on the CIFAR10 dataset in Sec. 5 of the paper. Here we also show that similar visual meanings can be drawn from intermediate nodes of larger trees such as the one for CIFAR100. Figure 14 displays the tree visualization for a WideResNet28x10 architecture on CIFAR100 (same model listed in Table 1 of Sec. 4.2). It can be seen in Figure 14 that subtrees can be grouped by visual meaning, which can be a Wordnet attribute like *Vehicle* or *Household Item*, or a more contextual meaning such as shape or background like *Cylindrical* or *Blue Background*.

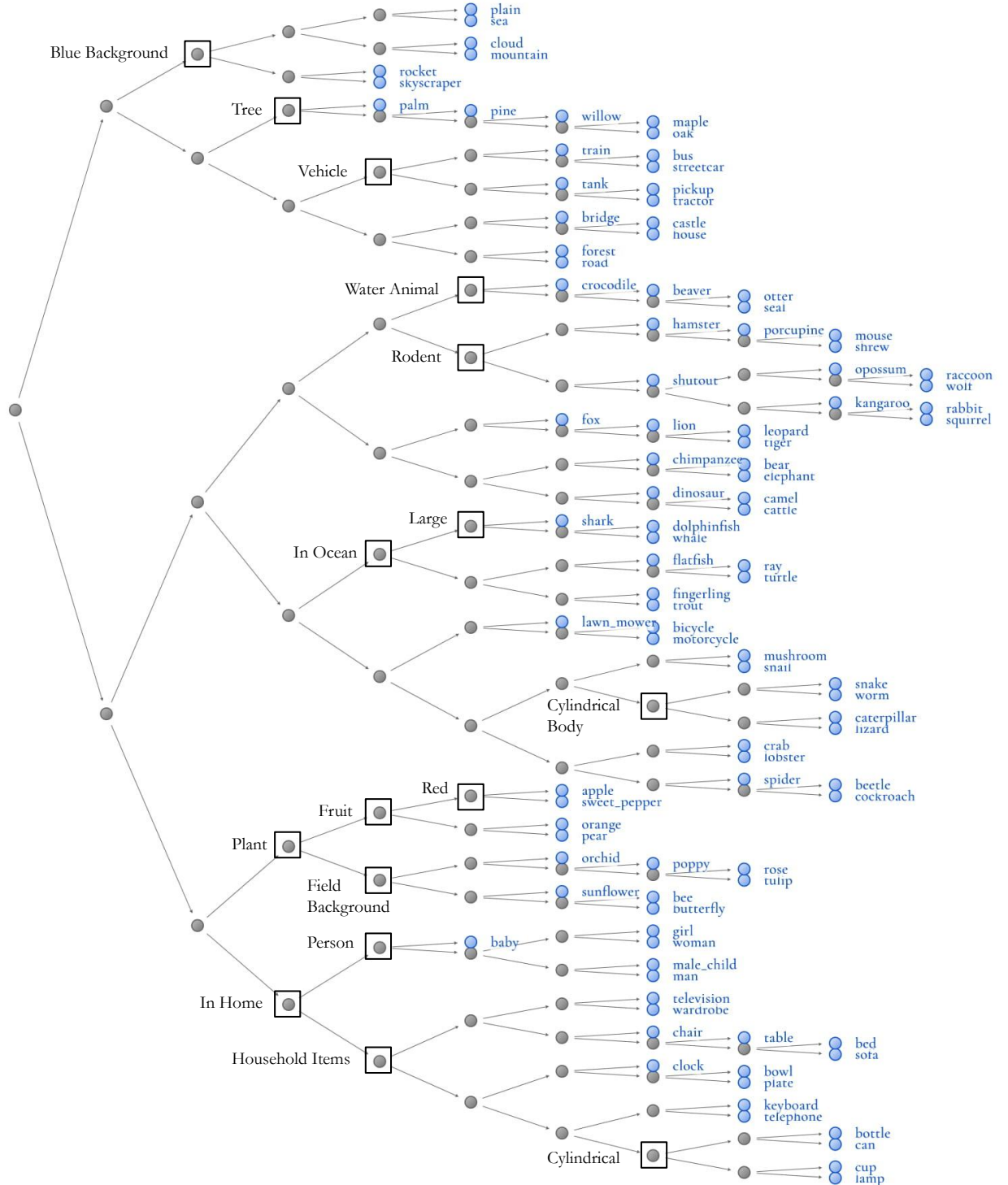


Figure 14: CIFAR100 tree visualization on WideResNet28x10 with samples of intermediate node hypothesis. Some nodes split on Wordnet attributes while other split on visual attributes like color, shape, and background.